CHEMICAL STABILITY OF THERMAL INSULATING MATERIALS IN SODIUM VAPOUR ENVIRONMENT

Raymond Luneng[1], Søren N. Bertel[2], Jørgen Mikkelsen[2], Arne P. Ratvik[3], Tor Grande[1]

1. Department of Materials Science and Engineering, NTNU, Norwegian University of Science and Technology, NO-7491 Trondheim, Norway.
2. Skamol A/S, Østergade 58-60, 7900 Nykøbing Mors, Denmark.
3. SINTEF Materials and Chemistry, NO-7465 Trondheim, Norway.
Corresponding author: raymond.luneng@ntnu.no

Keywords: Thermal Insulating Materials, Aluminium Electrolysis Cell, Sodium Vapour, Moler, Calcium Silicate, Vermiculite, Degradation.

Abstract

The most typical thermal insulating materials used in the cathode lining in aluminium electrolysis cells are Moler, calcium silicate, or vermiculite. The thermal insulation is important for the overall thermal and dimensional stability of the cell. The chemical stability of the thermal insulating materials is important, especially in cases where the refractory layer above the thermal insulation layer becomes fully penetrated by sodium vapour. The chemical degradation of thermal insulating materials by sodium vapours has been investigated in a laboratory test resembling the environments in the cathode lining. The exposed materials were investigated with respect to changes in the microstructure and chemical and mineralogical composition by a combination of optical and electronic microscopy and powder X-ray diffraction. These investigations revealed different reaction patterns for the three materials and the formation of new mineralogical phases were identified. Finally, these findings were compared with chemical reactions with sodium based on computational thermodynamics.

Introduction

The production of primary aluminium is an energy demanding process that takes place by molten salt electrolysis. Even today, the basic concept is very much the same as the one introduced in 1886 by the chemists Charles Martin Hall and Paul Louis Toussaint Héroult. However, the design and technology of the electrolysis cells are constantly evolving to yield higher productivity, and the industry has moved towards both high amperage cells, as well as low energy cells. In a modern cell, the sidewalls are designed with materials having high thermal conductivity in order to form a frozen layer of bath, the sideledge, which will protect the sidelining and potshell from the corrosive nature of the bath. The bottom of the cell, however, is designed with materials having low thermal conductivity, which will minimize the heat loss as well as reduce possible solidification of the bath towards the cathode. For low energy cells, the heat formation in the cell will be reduced and better insulation is needed to maintain operational temperatures. This may cause extra strain on the insulation materials, both from higher temperature at the interface between refractory and insulation materials, as well as chemical attack from penetrating volatile species and bath components.

The bottom insulation layer is most typically made of Moler (diatomaceous earth), calcium silicate, or vermiculite based materials [1]. The bottom lining is critical for both the thermal as well as the dimensional stability of the cell. The insulation materials have very poor resistance towards any bath components that may penetrate through the carbon cathode blocks, and therefore, a refractory layer is placed in between these two layers to protect the insulation from chemical attack by bath or volatile gases formed during electrolysis [1].

Under normal circumstances, the lifetime of modern cells is in most cases limited by the wear of the cathodes, which has become a major challenge with today's high amperage cells [2,3]. One way of increasing the cell lifetime is to increase the carbon cathode thickness, at the expense of the thickness of the refractory and insulation layers. Such new cell designs will put higher demand on the insulation layer and alter the thermal profile of the cell. In addition, volatile species such as Na and $NaAlF_4$ may penetrate the refractory layer and react with the highly porous insulation materials. Sodium vapour has been observed to be the first chemical species diffusing through the refractories [4,5]. The subsequent reaction with the bottom lining can alter the dimensional and thermal stability of the insulation materials, and ultimately change the performance of the electrolysis cell.

Moler, calcium silicate, and vermiculite based materials used in the aluminium industry were subject to sodium vapour exposure at elevated temperatures in a laboratory test inspired by Allaire et al. [6]. Both pristine materials and sodium exposed samples were investigated by a combination of optical and electron microscopy, as well as powder X-ray diffraction.

Experimental

The insulation materials investigated were Moler (SUPRA), calcium silicate (SUPER-1100 E), and vermiculite (V-1100 (475)), products by Skamol A/S. The weight and dimensions of the pristine samples, prior to sodium exposure, are given in Table 1.

Table 1. Dimensions and weight of the pristine insulation materials, prior to the sodium vapour test.

	H [mm]	W [mm]	L [mm]	M [g]	Density [kg/m^3]
Moler	50.2	48.7	149.6	285.8	781.4
Calcium Silicate	60.2	50.8	181.3	142.8	257.6
Vermiculite	60.4	51.1	179.6	255.5	460.9

The typical chemical composition of the pristine materials, as a product average by X-ray fluorescence measurements, are provided in Table 2. The chemical composition data has been collected from the materials data sheets. The weight and dimensions were

Table 2. Typical chemical composition of the insulation materials investigated, from the respective data sheets, given in wt%.

Product	SiO_2	Al_2O_3	Fe_2O_3	MgO	CaO	Na_2O	K_2O	SO_3	TiO_2	LOI*
SUPRA (Moler)	77	9.0	7.0	1.3	0.8	0.4	1.6	1.0	0.7	1.0
SUPER-1100 E (calcium silicate)	47	0.3	0.3	0.6	43	0.1	0.1	N/A	N/A	8
V-1100 (475) (vermiculite)	46	7.0	5.5	19.0	3.5	0.2	10.0	N/A	0.7	7.0

LOI*: Loss on ignition given at 1025 °C.

measured before and after the sodium vapour test. The bar shaped materials were placed inside a steel box with the surfaces facing a carbon crucible, as illustrated in Figure 1. 200 g NaF and 100 g Al were used as reactants in the carbon crucible to form cryolite and sodium vapour, by Equation (1).

$$6\ NaF(s) + Al(l) = Na_3AlF_6(s) + 3\ Na(g) \qquad (1)$$

The steel box was put in an oven, heated to 970 °C, and held for 48 h. The Moler material was heated to 850 °C, due to a limited service temperature of 950 °C. The test exposed the insulation materials to much greater sodium vapour pressures than can be expected under normal operating conditions in the electrolysis cell, and must be seen as an accelerated test procedure.

The three insulation materials are manufactured in different ways, and the Moler material is the only material that is exposed to temperatures close to normal operating temperatures during the production process. Therefore, the loss on ignition (LOI) for the Moler material is much lower compared to the calcium silicate and vermiculite based materials, as seen in Table 2. A thermal reference sample for the different materials were made by exposing them to the same temperature and length as the sodium vapour test, but without sodium exposure.

A bar of approximate dimensions of 5x1x1 cm^3 was cut from the upper part of the materials at the side closest to the carbon crucible, as illustrated with a red square in Figure 1. The material was crushed, sieved, and X-ray diffraction patterns of the materials were recorded using a Bruker AXS D8Focus X-ray diffractometer.

Figure 1. Setup for the sodium vapour test with the materials facing the carbon crucible holding the reactants. The red square indicates the part cut out and used for X-ray diffraction analysis. The lower right picture shows a horizontal cross section cut from the sodium exposed vermiculite material.

A horizontal cut of approximate height of 1 cm was made at the top of each bar, as illustrated in the lower right corner of Figure 1 for the V-1100 (475) vermiculite material. The specimens were broken to create fracture surfaces to be investigated by scanning electron microscopy, SEM (Hitachi S-3400N). Both secondary electrons and back-scattered electrons were used for SEM imaging.

Results

The macroscopic appearance of the pristine insulation materials changed significantly after sodium exposure in the laboratory test, as seen in Figure 2. Pristine materials are shown in the left pictures, and sodium exposed materials in the middle and right pictures.

Figure 2. From top to bottom: Moler SUPRA, SUPER-1100 E calcium silicate, and V-1100 (475) vermiculite. The left picture of each material shows the pristine material, while the others show the material after the sodium vapour test. The middle pictures show the side of the bar facing the carbon crucible.

The Moler material (upper three pictures in Figure 2) changed from an orange colour to brown/grey, with a darker side facing the carbon crucible during the test. The calcium silicate material (middle three pictures in Figure 2) changes colour from grey to white before and after heat treatment (thermal reference sample not

Table 3. The dimensions, weight, density, and mass difference observed for the materials before and after the sodium test, as well as before and after the thermal reference test.

Material	H [mm]	W [mm]	L [mm]	m [g]	Density [kg/m^3]	Diff. mass [wt%]
SUPRA pristine	50.2	50.0	149.5	295.6	787.8	N/A
SUPRA thermal ref.	50.0	49.9	149.0	293.6	789.8	- 0.7
SUPRA pristine	50.2	48.7	149.6	285.8	781.4	N/A
SUPRA sodium test	49.6	48.0	147.8*	279.6*	794.6*	- 2.2*
SUPER-1100 E pristine	60.0	51.1	180.4	142.1	256.9	N/A
SUPER-1100 E thermal ref.	59.3	50.5	179.4	126.3	235.1	- 11.1
SUPER-1100 E pristine	60.2	50.8	181.3	142.8	257.6	N/A
SUPER-1100 E sodium test	N/A**	N/A**	N/A**	132.6	N/A**	- 7.1
V-1100 (475) pristine	60.4	50.7	179.9	277.8	504.3	N/A
V-1100 (475) thermal ref.	59.5	50.5	177.7	260.8	488.4	- 6.1
V-1100 (475) pristine	60.4	51.1	179.6	255.5	460.9	N/A
V-1100 (475) sodium test	58.4	49.0	176.5	245.7	486.5	- 3.8

*: The bottom part of the sample was stuck to the steel box, giving errors in these values.
**: Unable to measure due to material deformation, as seen in Figure 2.

shown). Black areas and spots are observed after sodium exposure. The vermiculite material (bottom three pictures in Figure 2) has a pronounced gradient on the side facing the carbon crucible during the test. As seen in the lower right corner of Figure 1, the side facing the carbon crucible has changed colour. This part is close to 1 cm thick.

The changes in dimensions and weight of the materials after the test are provided in Table 3. The weight loss was lower for the sodium exposed samples compared to the thermal reference samples, pointing to reactions with sodium in the material during the experiments. A small part of the bottom of the Moler SUPRA sample was stuck to the steel box after the test, thus not providing the correct weight of the sample. For the SUPER-1100 E calcium silicate material, the sodium exposed sample had a weight loss of about 4 wt% less than the thermal reference. The V-1100 (475) vermiculite material had a weight loss of about 2 wt% less than the thermal reference. The calcium silicate material was heavily deformed after the test, demonstrating thermally activated creep.

X-ray Diffraction

The XRD measurements revealed different phases for the pristine samples, the thermal reference samples, and the sodium vapour exposed samples for all three materials, as illustrated in Figures 3-5. The XRD results for the Moler material is shown in Figure 3.

Moler is burned at high temperatures during manufacturing and therefore no difference was observed between the pristine and the thermal reference materials. The large broad feature in the XRD patterns for the Moler material points at the presence of amorphous or nano-crystalline phases. The main phases in the pristine and thermal reference materials are SiO_2, and Fe_2O_3. After sodium exposure, SiO_2 is still present, while Fe_2O_3 has disappeared. A new phase, $Mg_2Al_4Si_5O_{18}$, seems to be formed. However, the amount of amorphous phases in the Moler material is substantial when compared to the amount of crystalline phases.

The XRD pattern of the pristine calcium silicate material (Figure 4) show that xonotlite, $Ca_6Si_6O_{17}(OH)_2$, is present. However, after thermal treatment the main phase is identified as wollastonite, $CaSiO_3$. The X-ray pattern of the sodium exposed sample demonstrates that the main phase after sodium exposure is $Na_2Ca_2Si_2O_7$, a sodium calcium silicate. Combeite, $Na_2Ca_2Si_3O_9$, was also found in the exposed material.

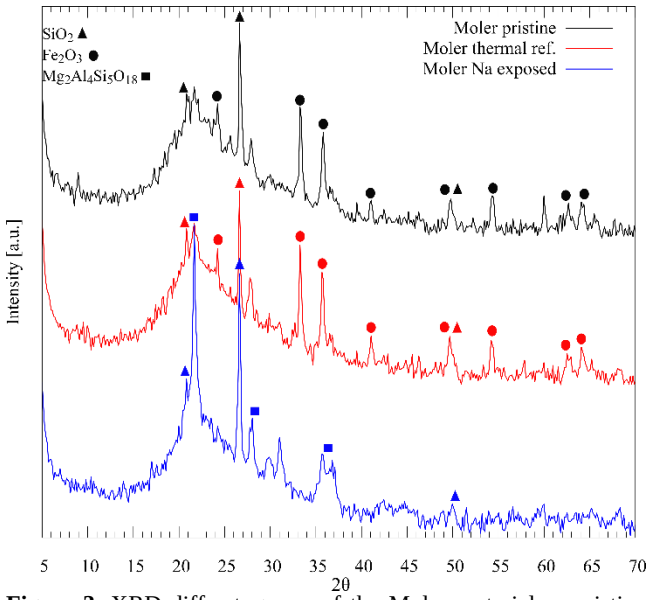

Figure 3. XRD diffractograms of the Moler material as pristine sample (upper black graph), thermal reference sample (middle red graph), and sodium exposed sample (lower blue graph). The most important phase peaks are also marked.

The XRD measurements of the vermiculite material are shown in Figure 5. The X-ray pattern of the pristine vermiculite sample show the main phase to be vermiculite, $(Mg,Fe^{+2},Fe^{+3})_3[(Al,Si)_4O_{10}](OH)_2{\cdot}4H_2O$, a hydrated magnesium aluminium silicate mineral. After the heat treatment, forsterite, Mg_2SiO_4, and leucite, $KAlSi_2O_6$, phases were also observed. Forsterite is identified in the sodium exposed sample, together with a sodium aluminium silicate oxide, $NaAlSiO_4$, and $KAlSiO_4$, as the main phases.

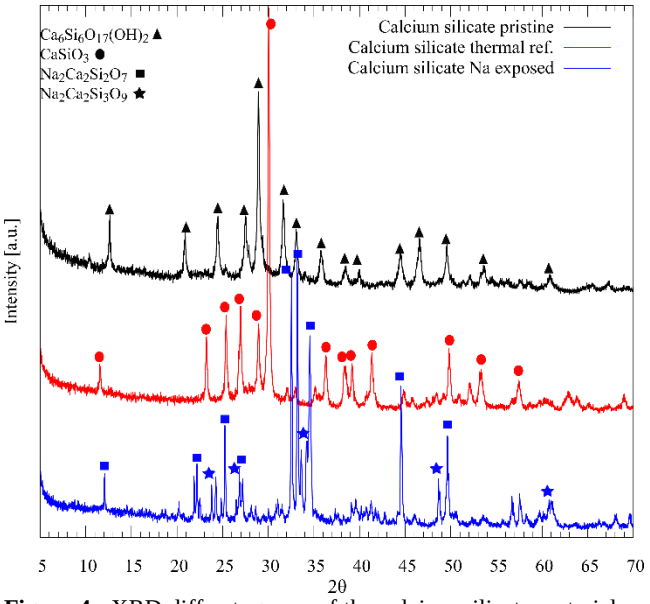

Figure 4. XRD diffractograms of the calcium silicate material as pristine sample (upper black graph), thermal reference sample (middle red graph), and sodium exposed sample (lower blue graph). The most important phase peaks are also marked.

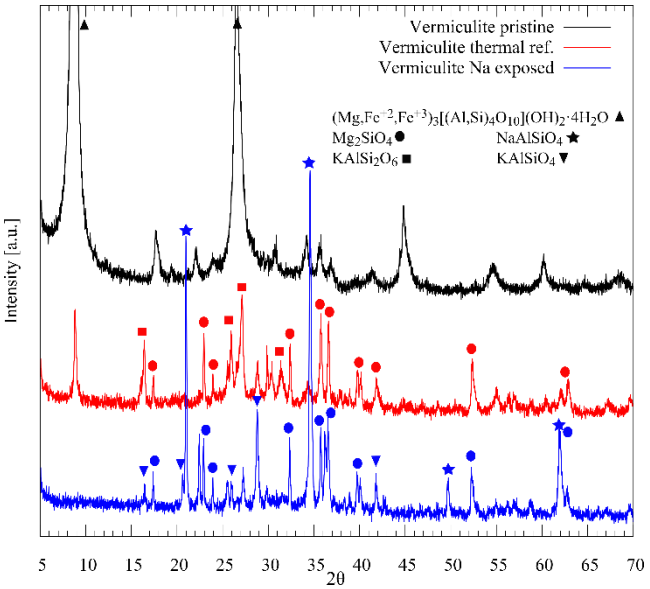

Figure 5. XRD diffractograms of the vermiculite material as pristine sample (upper black graph), thermal reference sample (middle red graph), and sodium exposed sample (lower blue graph). The most important phase peaks are also marked.

Scanning Electron Microscopy

The microstructure of the pristine materials are compared with the microstructure of the exposed materials, shown in Figure 6. The porous nature of the three pristine materials are evident by the SEM images to the left. The mechanisms for obtaining high porosity in the three materials are in principle different and the microstructures are quite different, but all three are highly porous.

The image of the sodium exposed Moler material (upper pictures in Figure 6) revealed a thin glassy layer on the side facing the carbon crucible during the test. Although not continuous, it covers the surface quite well, as seen from the top down view. The calcium silicate material is still highly porous, but the microstructure has coarsened during the sodium test, reflecting the macroscopic change in shape due to creep. The pristine vermiculite material is mostly exfoliated vermiculite grains pressed together with a water glass binder. The sheet structure of the grains in the pristine material is clearly seen by SEM imaging. After sodium exposure, this characteristic microstructure is not observed, reflecting that the reaction with sodium leads to significant coarsening of the grains and remove the fine porous microstructure.

Discussion

From the XRD data, the following phase changes are proposed for the Moler material. The pristine sample and the thermal reference sample have the same phase compositions since the Moler material is burned at high temperatures during manufacturing. After sodium exposure the iron oxide, Fe_2O_3, has disappeared due to the reactions and is likely reduced to a different phase with Fe^{2+}. A glassy phase is formed on the side facing the carbon crucible, which is also observed by SEM. The SiO_2, and $Mg_2Al_4Si_5O_{18}$ phases are still present, while the major part of the material remains amorphous. From SEM imaging, and preliminary energy-dispersive X-ray spectroscopy (EDS) measurements (not reported here), the glassy layer that is formed seems to be quite thin, but high in sodium content, most likely forming a viscous sodium aluminosilicate liquid, which turns into a glass during cooling. The sodium content drops significantly beyond this layer and further inside the material.

Recent work on thermodynamic stability of thermal insulating materials in sodium vapour environment [7] predicts both SiO_2, and $Mg_2Al_4Si_5O_{18}$ phases to be present in the Moler material at low sodium content. Albite, $NaAlSi_3O_8$, is also predicted to increase significantly with increasing sodium content. Glassy phases (or liquid at elevated temperatures) close to albite, which normally does not crystallize, have previously been reported to be present in reacted refractory layers of shut down cells [5]. The bar shrunk in all three dimensions during the test, but due to a small part of the bottom being stuck to the steel plate, the length and weight measurements reported are not accurate. Thus, no conclusions can be drawn about the macroscopic difference in wt% compared to the thermal reference sample. However, based on the sodium content in the outer layer, some sodium uptake is likely. The attachment of the sample to the steel plate also points to the formation of a viscous liquid due to reactions with sodium.

From the XRD data, the following is proposed for the calcium silicate material. During heat treatment, the calcium silicate material transforms from xonotlite to wollastonite, by evaporation of water. When exposed to sodium, the wollastonite reacts to form both $Na_2Ca_2Si_3O_9$ and $Na_2Ca_2Si_2O_7$. By thermodynamic equilibrium calculations, $Na_2Ca_2Si_3O_9$ is predicted to form by increasing sodium content, while $Na_2Ca_2Si_2O_7$ is not predicted [7]. The experimental results therefore point to kinetics being important for the phase transformations and reaction with sodium. Elemental silicon is also predicted to form by thermodynamic calculations [7], but has not been identified so far and calls for further investigations. However, the black colour on the sodium exposed calcium silicate material may possibly come from the formation of silicon, but this

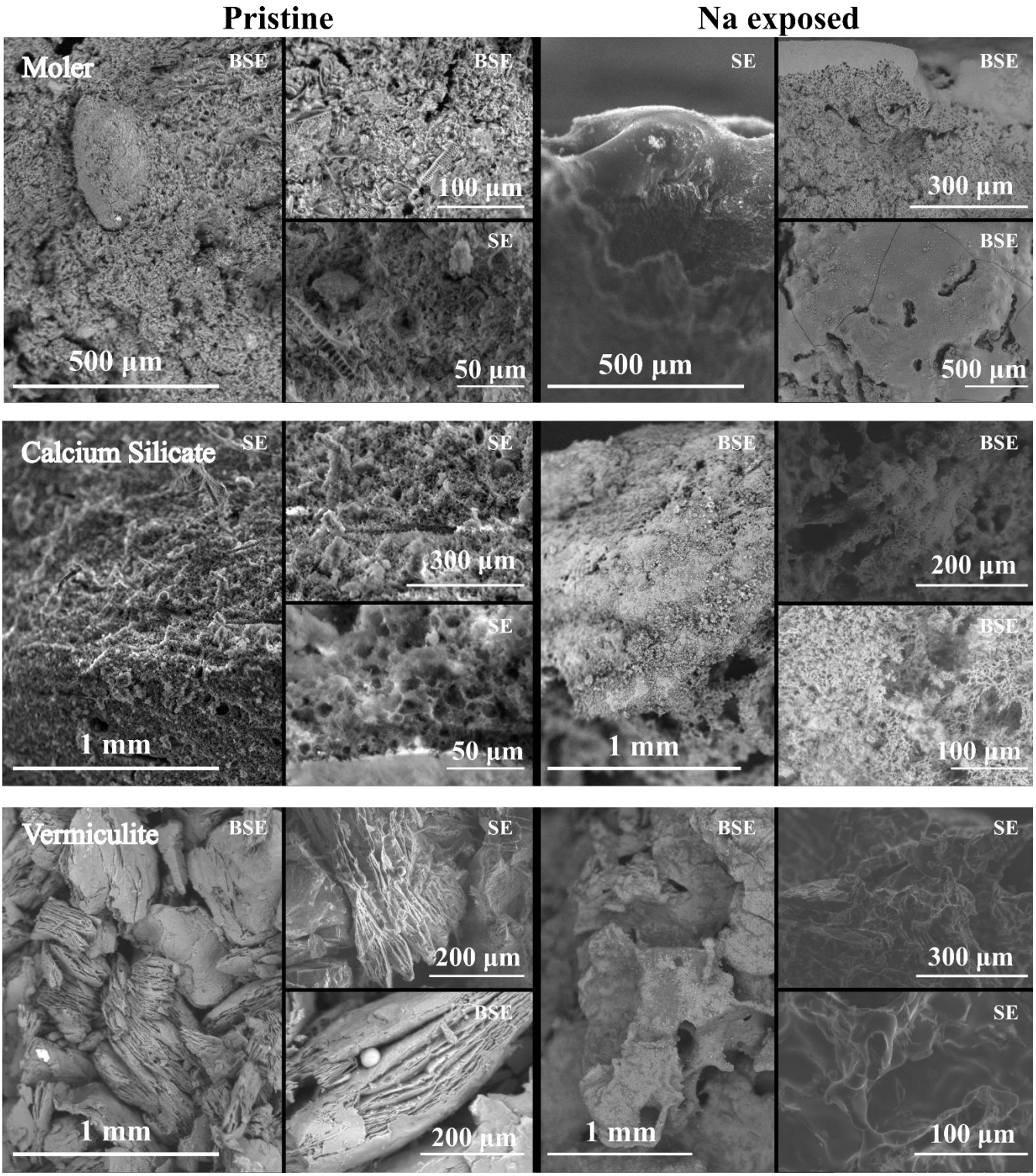

Figure 6. SEM images of the pristine materials to the left, and sodium exposed samples to the right. Note that some images are from secondary electrons (marked SE) and some are back-scattered electrons (marked BSE). From top to bottom: Moler SUPRA, SUPER-1100 E calcium silicate, and V-1100 (475) vermiculite. For the Moler sample, a thin glassy layer is observed after sodium exposure, as seen in the upper right pictures. A top down view is also provided, which illustrates that the glassy layer is not continuous across the surface. The organic fibres, seen in the pristine calcium silicate sample, burn off during the test, and the sodium exposed sample show more of a dendritic structure and large voids/pores. The exfoliated grains of the pristine vermiculite can clearly be seen in the lower left pictures, where the grains open up in parallel sheets. This structure is lost during sodium exposure, and a more continuous phase is observed.

is yet to be confirmed. The calcium silicate material suffered severe deformation during the test, as is seen in Figure 2, with no external load except the weight of the bar itself. In light of the SEM images, it is still showing a rather porous structure, which points to deformation by creep that is, most likely caused by viscous flow. A coarsening of the microstructure is also observed. The XRD data also show complete mineralogical transformations taking place comparing the patterns of the pristine, the thermal reference, and the sodium exposed material. This points to an inability of the material to resist sodium infiltration, as opposed to the Moler material where a complete phase transformation is not observed, and a glassy layer is formed. Compared to the thermal reference sample, the sodium exposed calcium silicate sample had an approximate 4 wt% increase, pointing to a high uptake of sodium in the material.

For the vermiculite material, the thermal treatment of the reference sample leads to formation of forsterite, Mg_2SiO_4, and leucite, $KAlSi_2O_6$, illustrating that the material is not thermally stable with respect to phase composition. After sodium exposure, forsterite is still present, together with $NaAlSiO_4$, and $KAlSiO_4$, as the main phases. These phases have also been predicted to coexist by thermodynamic equilibrium calculations at moderate sodium content [7]. Compared to the thermal reference sample, the sodium exposed sample had an approximate 2 wt% increase, about half of what was observed for the calcium silicate material. SEM imaging revealed a distinct difference between the macroscopic gradient observed in the lower right picture of Figure 1. While the inner part has a structure similar to the pristine material, with exfoliated vermiculite grains (lower left pictures of Figure 6), the porous sheet structure of the grains is not seen in the outer part (lower right pictures of Figure 6). Preliminary EDS measurements (not reported here) also show high sodium content in the outer part. The material shrunk in all dimensions, but as opposed to the calcium silicate material, it did not deform dramatically and is apparently retaining its structural integrity. By the XRD and SEM data, the vermiculite material does not create a glassy barrier layer like the Moler material, nor does it experience a complete mineralogical transformation like the calcium silicate material. Instead, the sodium vapour penetrates the outer layer and reacts with the material, leaving the inner layer, more or less, intact.

Lastly, it is worth mentioning that in a typical design of an aluminium electrolysis cell, the Moler material (SUPRA) and vermiculite material (V-1100 (475)) are usually located in the upper part of the insulation layer, thus being closest to the refractory layer and the cathode. The calcium silicate material (SUPER-1100 E) is used as back-up insulation, in the bottom part of the insulation layer. In light of the results, this placement is most beneficial, as the Moler and vermiculite materials are seen to tolerate higher sodium vapour exposure much better than the calcium silicate material.

Conclusion

A laboratory scale test was set up to expose three common thermal insulating materials to sodium vapour, which is likely the first volatile specie to diffuse through the refractory layer of aluminium electrolysis cells. Phase transformations during a reference heat treatment were observed in the calcium silicate and vermiculite materials, but not in the Moler material. When exposed to sodium vapour in the test, the Moler material reacts to form a glassy layer, which limits further penetration of sodium. A complete phase transformation occurs in the calcium silicate material, and severe deformation by creep is observed. The vermiculite material maintains its structural integrity, but sodium penetrates deeper inside the material than in the case of the Moler material.

Acknowledgement

Financial support from the Norwegian Research Council and Hydro Aluminium, Alcoa Norway, Elkem Carbon, and Skamol A/S, through the project CaRMa - Reactivity of Carbon and Refractory Materials used in Metal Production Technology, is gratefully acknowledged.

References

1 A. Seltveit, *Ildfaste materialer* (Trondheim, NO: Tapir, 1992).

2 E. Skybakmoen, A.P. Ratvik, A. Solheim, S. Rolseth, H. Gudbrandsen, "Laboratory test methods for determining the cathode wear mechanism in aluminium cells," *Light Metals*, 2007, 815–820.

3 K. Tschöpe, A. Store, S. Rorvik, A. Solheim, E. Skybakmoen, T. Grande, A.P. Ratvik, "Investigation of the Cathode Wear Mechanism in a Laboratory Test Cell," *Light Metals*, 2012, 1349–1354.

4 K. Tschöpe, C. Schøning, J. Rutlin, T. Grande, "Chemical Degradation of Cathode Linings in Hall-Héroult Cells - An Autopsy Study of Three Spent Pot Linings," *Met. Trans. B*, 43 (2012) 290–301.

5 K. Tschöpe, J. Rutlin, T. Grande, "Chemical Degradation Map for Sodium Attack in Refractory Linings," *Light Metals*, 2010, 871–876.

6 C. Allaire, R. Pelletier, O.-J. Siljan, A. Tabereaux, "An improved corrosion test for potlining refractories," *Light Metals*, 2001, 245.

7 R. Luneng, T. Grande, A.P. Ratvik, "Assessment of the Thermodynamic Stability of Thermal Insulating Materials in Aluminium Electrolysis Cells," *Proc. 34th Int. ICSOBA Conf.*, (2016) 1–10.